PERGAMON

International Journal of Heat and Mass Transfer 45 (2002) 4305–4313

International Journal of HEAT and MASS TRANSFER

www.elsevier.com/locate/ijhmt

Non-Darcy effects in buoyancy driven flows in an enclosure filled with vertically layered porous media

A.A. Merrikh [a], A.A. Mohamad [b,*]

[a] Laboratory for Porous Materials Applications, Department of Mechanical Engineering, SMU Dallas, TX 75275-0337, USA
[b] Department of Mechanical Engineering, University of Calgary, Calgary, Alberta, Canada T2N 1N4

Received 18 June 2001; received in revised form 23 March 2002

Abstract

Natural convection in an enclosure filled with two layers of porous media is investigated numerically. Constant heat flux is imposed on the left vertical wall and the right wall is assumed to be at a low temperature. The focus of the work is on the validity of the Darcy model when various combinations of fluid Rayleigh number, Darcy number and permeability ratios are considered for fixed values of the modified Rayleigh numbers. It is found that the boundary effects (Brinkman term) have significant importance at higher modified Rayleigh numbers (Rayleigh number based on permeability, Ra_m). Calculations are performed for a modified Rayleigh number up to 10^5. The results showed that, for the investigated range of parameters, the flow structure and heat transfer could be different than what Darcy model predicts. Two circulations are predicted for $Ra_f = 1 \times 10^8$, for two different cases, $Da = 1 \times 10^{-3}$, $K_r = 1000$ and $Da = 1 \times 10^{-4}$, $K_r = 100$ ($K_r = K_1/K_2$). For $K_r > 1$, increasing permeability ratio decreases flow penetration from layer 1 to layer 2 while reverse is true for $K_r < 1$. For low Ra_m ($Ra_m \leqslant 10^3$) and $K_r = 1000$, the heat transfer is conductive in the right layer, while this is true for the left layer for $K_r = 0.001$. It is possible to obtain no-slip velocity boundary conditions both at the walls and at the interface between the porous layers even for very low permeability.

Keywords: Natural convection; Porous medium; Permeability ratio; Porous–porous interface; General flow model; Brinkman term; No-slip boundary condition

1. Introduction

Convection in porous media has gained significant attention because of its importance in engineering applications such as geothermal systems, solid matrix heat exchangers, thermal insulation, oil extraction and store of nuclear waste materials. Convection in porous media can be applied to underground coal gasification, ground water hydrology, iron blast furnaces, wall cooled catalytic reactors, solar power collectors, energy efficient drying processes, cooling of nuclear fuel in shipping flasks, water storage bays and natural convection in earth's crust. Reviews of the applications related to convective flows in porous media can be found in [1,2].

Especially in oil extraction process, oil flow encounters different layers of sand, rocks and limestone. Similar situations arise in geothermal reservoirs and acquifers [3,4]. There have been several attempts to study natural convection in a multi-layered porous media, including horizontal and vertical arrangements of the porous beds. Among those are the works of Rana [5], McKibbin and O'Sallivan [6,7], McKibbin and Tyvand [8], Poulikakos and Bejan [9] and Lai and Kulacki [10,11]. The above mentioned investigations are based on the Darcy's flow model.

Experiments have been conducted on porous media by combination of several fluids and porous beds including various ranges of governing parameters [12,13]. The experimental results are not in good agreement with prediction of the Darcy model except for a limited range

* Corresponding author. Tel.: +1-403-220-2781; fax: +1-403-282-8406.
E-mail address: amohamad@enme.ucalgary.ca (A.A. Mohamad).

0017-9310/02/$ - see front matter
PII: S0017-9310(02)00135-7

Nomenclature

A	aspect ratio
a, b	Ergun's empirical constants
Da	Darcy number (K_1/H)
F	inertia coefficient ($=b\phi^{-3/2}/\sqrt{a}$)
g	gravitational acceleration vector (m^2/s)
H	enclosure height (m)
k	thermal conductivity
K	permeability of the porous matrix
K_r	permeability ratio ($=K_1/K_2$)
Nu	Nusselt number
Pr	Prandtl number ($-v_f/\alpha_{eff}$)
Pr_m	modified Prandtl number ($=\sigma\phi Pr$)
q	heat flux
Ra	Rayleigh number ($=g\beta qH^4/\alpha_{eff}v_f k_{eff}$)
Ra_m	modified Rayleigh number ($=Kg\beta qH^4/\alpha_{eff}v_f k_{eff}$)
t	time (s)
T	temperature
$\boldsymbol{u}$	mean velocity ($=\sqrt{u^2+v^2}$)
$\boldsymbol{U}$	mean nondimensional velocity ($=\sqrt{U^2+V^2}$)
u	velocity in x-direction (m/s)
U	nondimensional velocity in x-direction ($=uH/\alpha_{eff}$)
v	velocity in y-direction (m/s)
V	nondimensional velocity in y-direction ($=vH/\alpha_{eff}$)
x	horizontal coordinate (m)
y	vertical coordinate (m)

Greek symbols

α	thermal diffusivity (m^2/s)
β	thermal expansion coefficient
ΔT	temperature difference
ϕ	porosity
Λ	inertial parameter ($F\phi^2\sigma H/\sqrt{K}$)
η	nondimensional coordinate in y-direction ($=y/H$)
μ	viscosity (kg m^{-1} s^{-1})
v	kinematic viscosity
θ	nondimensional temperature ($T-T_c/(qH/k_{eff})$)
ρ	density (kg/m^{-3})
σ	thermal capacity ratio
ξ	nondimensional coordinate in x-direction ($=x/H$)

Subscripts

1	physical properties that belong to the left porous layer
2	physical properties that belong to the right porous layer
av	average
c	cold
aff	effective properties related to saturated porous medium
f	fluid
r	ratio

of parameters (low Rayleigh numbers and for glass beads saturated with water). Also, the experimental results show that the Nusselt number depends not only on the modified Rayleigh number and the aspect ratio, but also on the fluid Rayleigh number, Darcy number, Prandtl number, inertia parameter and the thermal conductivity ratio between the fluid and solid phases. To our knowledge, non-Darcy model has not been used in analyzing buoyancy-induced flows in layered porous media.

The aim of the present study is to emphasize on the natural convection in an enclosed vertically layered saturated porous system subjected to a constant heat flux from one side and cooled from another side. By adapting the general flow model that includes both the Forchheimer and Brinkman terms, present work aims to investigate the effect of fluid Rayleigh number, Darcy number and permeability ratio on fluid flow and heat transfer. It is assumed that the fluid and porous beds are in local thermal equilibrium. The model equations are solved numerically by a second order accurate scheme. The results are represented for the fluid Rayleigh number between 10^6–10^8 and permeability ratios of 0.001 to 1000 for the Darcy number ranging between 10^{-7} and 10^{-1}. The selected range of the Darcy numbers in the present study include very high values ($Da > 10^{-4}$). Knowing that snow, lava, foam and limestone are of very high void fractions ($\phi > 90\%$), the selected values are necessary in order to carry out a parametric study. The Prandtl number as well as the inertia coefficient and the conductivity ratios between the two layers are assumed to be unity. The aim of the present study is to focus on the effects of fluid Rayleigh number, Darcy number and the permeability ratio on the flow field, heat transfer rate and interface conditions. Thus the conductivity ratio between the porous layers is set to unity. It is found that Darcy model fails to predict flow structure and heat transfer for high fluid Rayleigh and/or Darcy numbers. For high Ra_m ($\geqslant 1000$), Darcy model over-predicts the value of average Nusselt number because of boundary effects encountered both at the solid walls and at the interface between the porous

layers. It will be shown that for $Da \geqslant 10^{-5}$, no-slip boundary conditions exist not only at the solid walls, but also on the interface between the two layers. It will be shown that no-slip conditions also depend on the permeability ratio.

2. Model equations

Incompressible, two-dimensional, laminar natural convection in a square (aspect ratio of unity) enclosure filled with homogeneous, saturated, isotropic porous medium with constant thermo-physical properties except the density variation in the buoyancy term is studied numerically. It is assumed that the solid matrix and the fluid are in local thermal equilibrium. The enclosure is filled with two vertically layered porous media, having different permeability. The equations that govern the conservation of mass, momentum and energy equations as suggested by [1] can be written as follows

$$\nabla \cdot u = 0 \tag{1}$$

$$\frac{\rho_f}{\varepsilon}\left(\frac{\partial u}{\partial t} + u\frac{\partial u}{\partial x} + v\frac{\partial u}{\partial y}\right) = -\frac{\partial p}{\partial x} + \mu_{\text{eff}}\nabla^2 u - \frac{\mu_{\text{eff}}}{K}u - \frac{\rho c_F \varepsilon}{\sqrt{K}}|\boldsymbol{u}|u \tag{2}$$

$$\frac{\rho_f}{\varepsilon}\left(\frac{\partial v}{\partial t} + u\frac{\partial v}{\partial x} + v\frac{\partial v}{\partial y}\right) = -\frac{\partial p}{\partial x} + \mu_{\text{eff}}\nabla^2 v - \frac{\mu_{\text{eff}}}{K}v - \frac{\rho c_F \varepsilon}{\sqrt{K}}|\boldsymbol{u}|v \tag{3}$$

$$\sigma\frac{\partial T}{\partial t} + u\frac{\partial T}{\partial x} + v\frac{\partial T}{\partial y} = \alpha_{\text{eff}}\nabla^2 T \tag{4}$$

Eqs. (2) and (3) are the transport equations including both the boundary and the inertial effects. Mass, momentum and energy are conserved at the interface between the porous beds. It should mention that inclusion of advection terms does not have any influence on the flow and temperature fields and can be neglected.

The continuity of horizontal and vertical flow, pressure and temperature can be expressed at the interface as, $u_1 = u_2$, $v_1 = v_2$, $p_1 = p_2$, $T_1 = T_2$. The conservation of vertical and horizontal stress [20] can be expressed as:

$$\mu_{\text{eff}}\left(\frac{\partial u}{\partial x}\right)_1 = \mu_{\text{eff}}\left(\frac{\partial u}{\partial x}\right)_2 \tag{5a}$$

$$\mu_{\text{eff}}\left(\frac{\partial v}{\partial x} + \frac{\partial u}{\partial y}\right)_1 = \mu_{\text{eff}}\left(\frac{\partial v}{\partial x} + \frac{\partial u}{\partial y}\right)_2 \tag{5b}$$

Energy at the interface is also conserved as:

$$k_{\text{eff}}\left(\frac{\partial T}{\partial x}\right)_1 = k_{\text{eff}}\left(\frac{\partial T}{\partial x}\right)_2 \tag{5c}$$

In the above equations, subscripts 1 and 2 refer to the left and right of the interface, respectively. The Eqs. (1)–(4) can be written in a dimensionless form as:

$$\nabla \cdot \boldsymbol{V} = 0 \tag{6}$$

$$\frac{\partial U}{\partial \tau} + U\frac{\partial U}{\partial \xi} + \boldsymbol{V}\frac{\partial U}{\partial \eta} = -\frac{\partial P}{\partial \xi} + Pr_m\nabla^2 U - \frac{Pr_m}{Da}U - \Lambda|\boldsymbol{U}|U \tag{7}$$

$$\frac{\partial V}{\partial \tau} + V\frac{\partial V}{\partial \xi} + V\frac{\partial V}{\partial \eta} = -\frac{\partial P}{\partial \eta} + Pr_m\nabla^2 V + Pr_m Ra\theta - \frac{Pr_m}{Da}V - \Lambda|\boldsymbol{U}|V \tag{8}$$

$$\frac{\partial \theta}{\partial \tau} + U\frac{\partial \theta}{\partial \xi} + V\frac{\partial \theta}{\partial \eta} = \nabla^2\theta \tag{9}$$

3. Boundary conditions

No slip condition is imposed on the solid walls, i.e., velocity components are set to zero. A uniform heat flux is applied at the left wall of the cavity, while the right vertical wall is kept at a low temperature. The horizontal walls are assumed to be adiabatic. The non-dimensional thermal boundary conditions can be expressed as follows:

$$\left.\frac{\partial \theta}{\partial \xi}\right|_{\xi=0} = 1 \tag{10a}$$

$$\theta|_{\xi=L} = 0 \tag{10b}$$

The average Nusselt number can be defined as

$$Nu_{\text{av}} = \frac{1}{\theta_m} \tag{11}$$

θ_m is the average temperature of the heated wall and is defined as:

$$\theta_m = \int_{\eta=0}^{\eta=1} \theta|_{\xi=0}\,\mathrm{d}\eta \tag{12}$$

4. Numerical procedure and grid independence

Second order accurate in space, MacCormack scheme, is adopted for the solution of the governing equations. The accuracy of the scheme and the method of its application for the solution of the incompressible convection–diffusion problems are explained in [14,17]. Staggered grid arrangement, together with MAC method [15] are adopted for the numerical solution of the

governing equations. In order to obtain grid independent results, different uniform grid numbers, 41×41, 81×81 and 141×141 are tested for $Ra_m = 100$, $Da = 1 \times 10^{-2}$ and $K_r = 100$. It is noticed that the difference between the results predicted based on 81×81 and 141×141 grids are insignificant (<1%). The average Nusselt number for the tested grid points was 3.152, 3.041 and 3.031 for grids 41×41, 81×81 and 141×141 respectively. Thus 81×81 grids are used for generating the results. Nusselt number on both vertical walls are equal, this is ensures that the energy is conserved globally.

For further assessment of the code, present results are tested and compared with Darcy model solutions of Refs. [11,16], as shown in Tables 1 and 2 respectively. Table 1 shows the comparison with a single porous layer subjected to a constant heat flux from a side. The results for $Ra_m \leqslant 1000$ agree well with the correlation suggested by Prasad and Kulacki [16]. Slight deviation of general model compared with Darcy model at high Ra_m are a result of boundary effects associated with the no-slip boundary conditions. For vertically layered media, present results show that there is good agreement between the present results and results of [11], Table 2. But at higher modified Rayleigh numbers, the deviation between the general model and Darcy model becomes significant due to the boundary effects.

Table 1
Comparison of present results with the Darcy model of Ref. [16]

Ra_m ($Ra_f \cdot Da$)	General model ($Da \leqslant 1 \times 10^{-5}$)	Results of Ref. [16] ($Nu_{av} = 0.312 Ra_m^{0.413}$)
100	2.11	2.09
200	2.78	2.78
500	4.05	4.06
1000	5.35	5.41
10 000	13.72	14.00

Table 2
Comparison of the present results with the results of Ref. [11]

Ra_m	K_r	Present results (General model)		Results of Ref. [11] (Darcy model)
1000	0.01	$Ra_f = 10^8$	7.28	8.05
		10^7	6.55	
		10^6	4.93	
1000	0.1	10^8	6.88	7.30
		10^7	6.68	
		10^6	4.86	
100	0.01	10^8	3.14	3.21
		10^7	3.02	
		10^6	2.97	
1000	10	10^7	3.00	3.00
		10^6	2.95	

5. Results and discussion

In the following paragraphs the flow structure and heat transfer will be discussed. The effect of permeability ratio, Darcy and Rayleigh numbers will be separately discussed. In order to have a fair comparison between the flow structure and heat transfer, Ra_m is fixed at the layer 1 as the permeability ratios are varied for $K_r = 10$–1000, while for $K_r = 0.1$–0.001, Ra_m is fixed at the layer 2.

5.1. Flow structure

5.1.1. Non-darcy effects

It is known that for the non-Darcy region, the fluid flow and heat transfer depend on the fluid Rayleigh number and the Darcy number if other parameters (Prandtl number, inertia parameter and conductivity ratio) are fixed Fig. 1. Thus, for a fixed modified Rayleigh number, different fluid Rayleigh numbers (or different Darcy numbers) result different flow structures and heat transfer for the non-Darcy regime. Fig. 2 shows the streamlines and isotherms for $Ra_m = 100$ and $K_r = 0.001$. It is evident from Fig. 2 that increasing the fluid Rayleigh number decreases the flow circulation at layer 1. Since the modified Rayleigh number is fixed, a lower fluid Rayleigh number is associated with a more permeable media (i.e. higher Darcy number). Thus the strength of the flow in the left layer (layer 1) increases by decreasing fluid Rayleigh number. Stronger flow at the right layer results flow stratification and parallel isotherms are formed in the right layer. For $Ra_f = 10^6$,

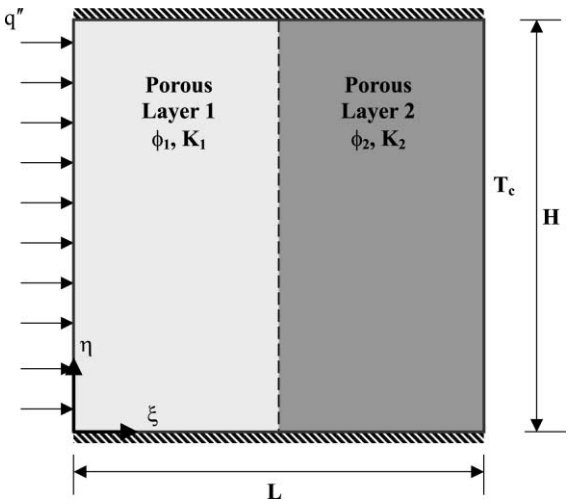

Fig. 1. Schematic of the layered porous media and the coordinate system.

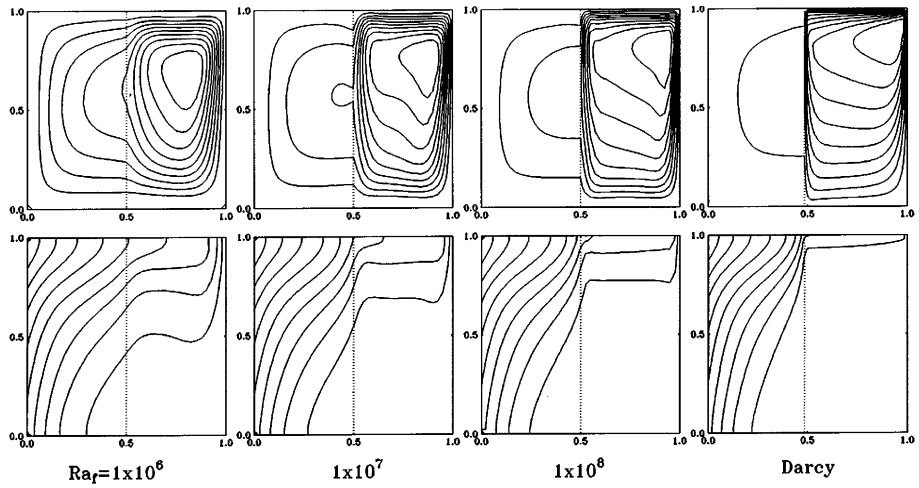

Fig. 2. Streamlines (top) and isotherms (bottom) for $Ra_m = 100$, $K_r = 0.001$.

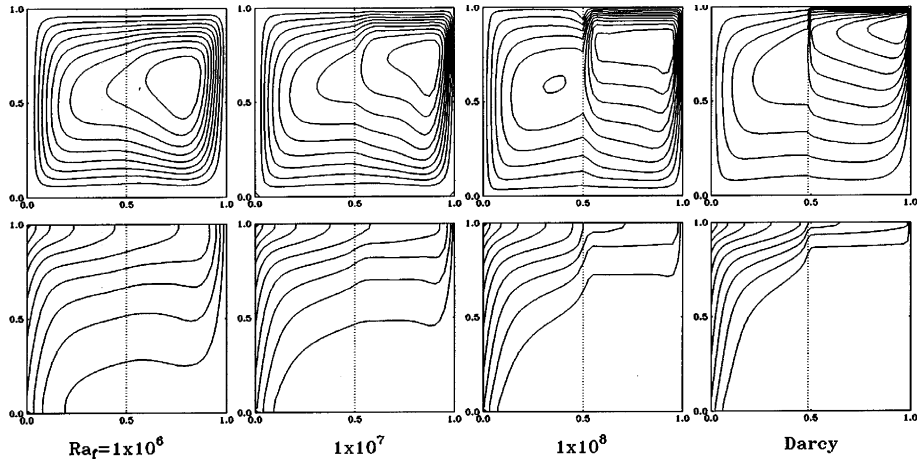

Fig. 3. Streamlines (top) and isotherms (bottom) for $Ra_m = 1 \times 10^3$, $K_r = 0.01$.

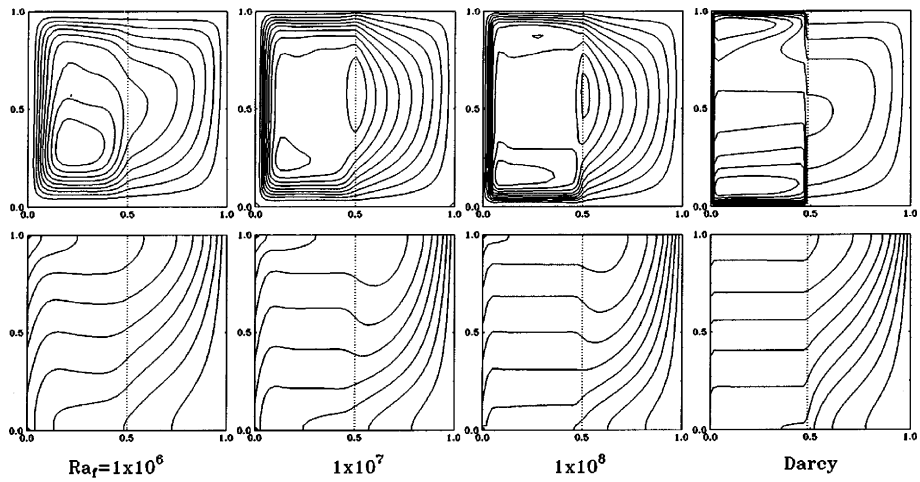

Fig. 4. Streamlines (top) and isotherms (bottom) for $Ra_m = 1 \times 10^5$, $K_r = 1000$.

isotherms are located down to mid-height of the enclosure as a result of high flow penetration from the left layer. But for Darcy flow, almost no temperature gradient exists in layer 1 due to high mixing mechanism in the right layer. The previous discussion can also be valid for $Ra_m = 1000$ and $K_r = 0.01$ being evident in Fig. 3. The flow penetration and recirculation enhances in both layers as the Ra_m increases from 100 to 1000 comparing Fig. 2 with Fig. 3.

Fig. 4 shows flow patterns and isotherms for $K_r = 1000$ and $Ra_m = 10^5$. The recirculating loop in the left layer locates in the lower left corner of the enclosure. Such flow patterns were also obtained by Beckermann et al. [18] both experimentally and theoretically for fluid/porous systems. For $Ra_f = 1 \times 10^8$ two circulating loops are formed, one located in the lower left corner and other at the center of the cavity. Darcy model shows two recirculating loops located at the bottom and top of the left layer. As a result of strong advection in the left layer, the thermal stratification in the left layer increases by increasing the fluid Rayleigh number. Also the boundary layer thickness decreases on the left boundary as the fluid Rayleigh number, Ra_f, increases, Fig. 5(a) and (b). Fig. 5(a) and (b) show quantitative results, i.e., velocity profiles for $Ra_m = 10^3$ and 10^5 respectively. As it can be seen from the figures, four distinct boundary layers exist. Two boundary layers along the two impermeable walls of the enclosure and other two boundary layers at the interface of the layers. Steep velocity changes occur at the interface for Darcy flow because of the slip conditions at the interface. For $Ra_m = 10^3$ and $Ra_f < 10^7$, the difference between the velocity profiles becomes less, compared to the higher modified Rayleigh numbers ($Ra_m = 10^5$), Fig. 5(a). Fig. 5(b) shows that at the right of the interface velocity peaks are formed both for $Ra_f = 1 \times 10^8$ and for the Darcy flow due to the flow recirculation. For $Ra_m = 10^3$ (Fig. 5(b)), the difference between prediction of the Darcy and general models is profound on the cold wall, while for $Ra_m = 10^5$ (Fig. 5(b)), the difference is profound on the heated wall. As mentioned earlier, previous investigators [3–11] have used Darcy model in their investigations. Then the results predicted by Darcy model may not be appropriate especially at the boundaries. Vafai and Thiyagaraja [19] claim that velocities at the interface between two porous media must be continuous and boundary layers are of no-slip type.

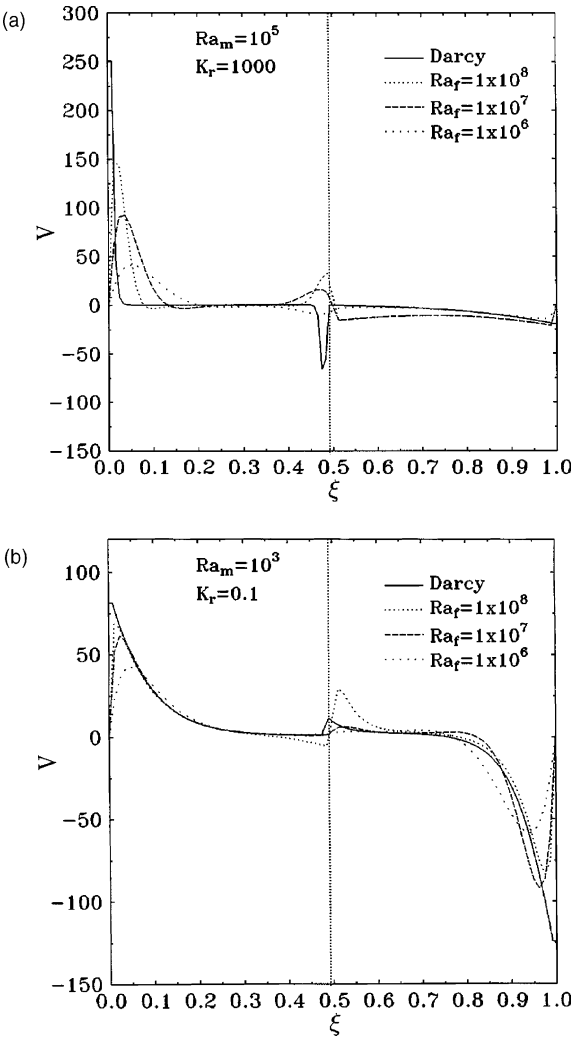

Fig. 5. (a) Variation of v-velocity at the mid-height of the enclosure for $Ra_m = 1 \times 10^5$ and $K_r = 1000$. (b) Variation of v-velocity at the mid-height of the enclosure for $Ra_m = 1 \times 10^3$ and $K_r = 0.1$.

5.1.2. Effect of permeability ratio

Generally, it is observed that if $K_r > 1$, decreasing the permeability ratio increases the flow penetration rate from layer 1 to layer 2, while reverse is true for $K_r < 1$. For such analysis, for $K_r > 1$, Darcy number at the layer 1 is fixed while for $K_r < 1$ Darcy number at layer 2 is fixed so that a fair comparison could be made between the permeability ratios. Fig. 6 shows streamlines and isotherms for $Ra_f = 1 \times 10^7$ for different permeability ratios. It is evident from Fig. 6 (1a) that the flow penetration into the right layer is minimal because of low permeability of layer 2 compared to layer 1. Hence the heat transfer is conductive in layer 2 (Fig. 6 (2a)). As K_r decreases, Fig. 6 (1b) and (1c), more flow penetrates into the layer 2 and advection effects increase in that layer. For $Ra_m = 10^4$ and $K_r = 10$, effect of permeability ratio is not that significant and strength of the flow in both layers becomes almost identical. For $K_r < 0.1$, however, layer 1 is less permeable and very small amount of flow penetrates into that layer, as shown in Fig. 6 (1e) and (1f). For $K_r = 0.001$, straight isotherms are formed in

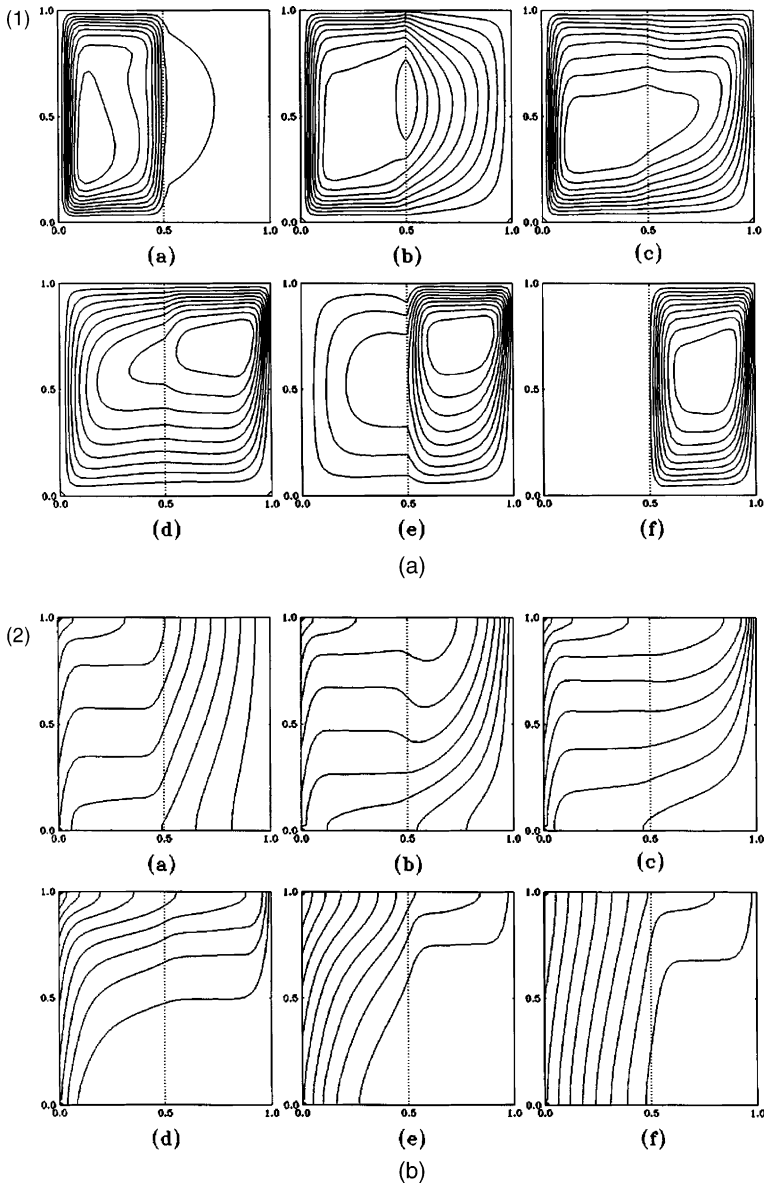

Fig. 6. (1) Streamlines (top) (2) isotherms (bottom) for $Ra_f = 1 \times 10^7$, $K_r =$ (a) 1000, (b) 100, (c) 10, (d) 0.1, (e) 0.01, (f) 0.001 (3) Variation of v-velocity at the mid-height of the enclosure for $Ra_f = 1 \times 10^7$ and $Da = 1 \times 10^{-3}$. (4) Variation of non-dimensional temperature with distance for $Ra = 1 \times 10^7$, $Da = 1 \times 10^{-3}$.

layer 1 as a result of conduction, Fig. 6 (2). There is isotherm stratification at the top of the layer 2 because of significant advection effects in that layer. For $K_r > 1$, it is more clear from Fig. 6 (3) that velocity at the mid-height of the cavity is almost zero at layer 2 for $K_r = 1000$. Fig. 6 (4) (shows that variation of temperature in this region is linear (conductive flow) because of very low velocities. Thus for $K_r = 1000$, layer 1 acts as a thin cavity with a thick right wall having same thermal conductivity as the porous medium. As the fluid Rayleigh number decreases, buoyancy forces decrease, and permeability gradients allow less amount of flow penetration.

5.2. Heat transfer

Non-Darcy effects are shown in Figs. 7 and 8. Figs. 7 and 8 show variation of average Nusselt number with permeability ratio for different modified Rayleigh numbers. It is evident that different combinations of Ra_f

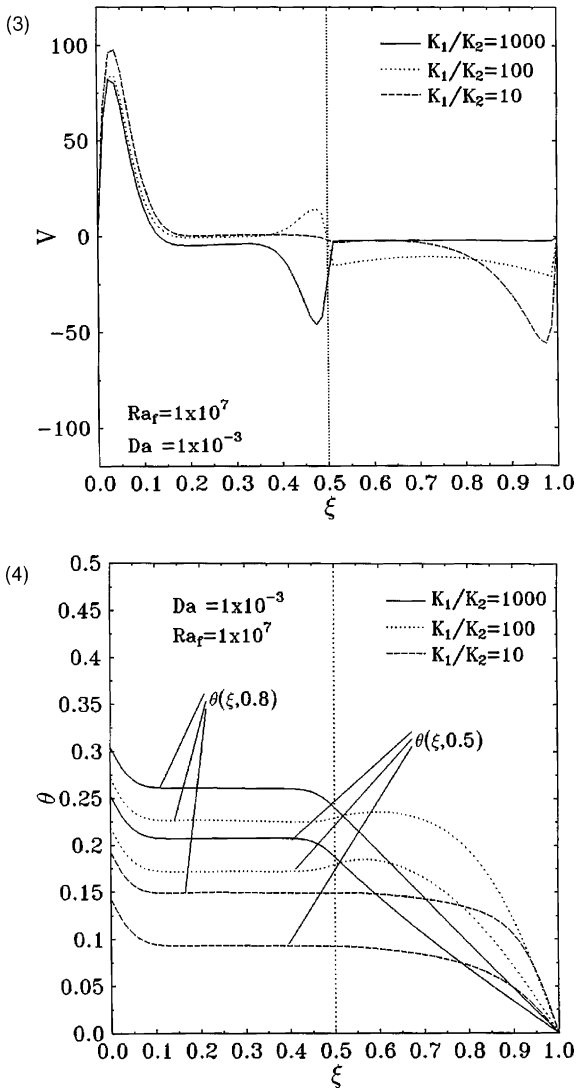

Fig. 6 (*continued*)

and *Da* result different heat transfer results. For a fixed Ra_m, higher Nusselt numbers are obtained for higher fluid Rayleigh numbers (lower Darcy numbers) compared to lower fluid Rayleigh. This shows the role of the fluid Rayleigh number in such phenomena. It is shown that Darcy model can be a limiting case for such a problem, since at very low permeabilities, the viscous terms are negligible compared to the Darcy term in the momentum equations. Brinkman term includes an additional (but in most cases realistic) diffusion into the transport equations and results in a decrease in heat transfer predictions of the general model when compared to the Darcy model. In a layered system, the inclusion of the viscous term results no-slip boundary

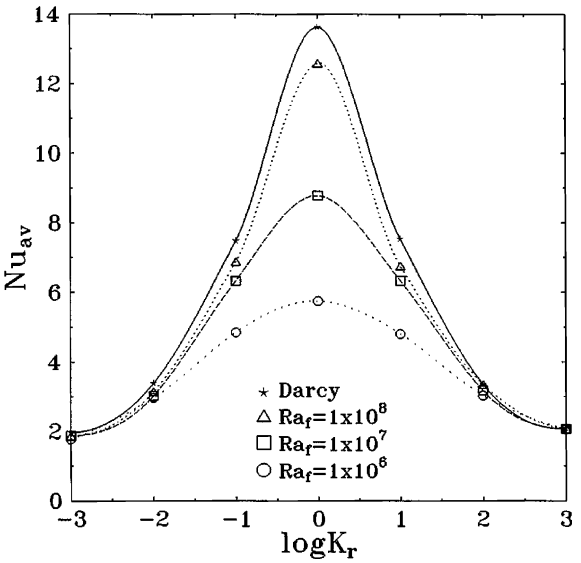

Fig. 7. Variation of Nu_{av} with permeability ratio $Ra_m = 10^4$ for $K_r > 1$ $Ra_m = 1000$, 100, 10 for $K_r = 0.1$, 0.01, 0.001.

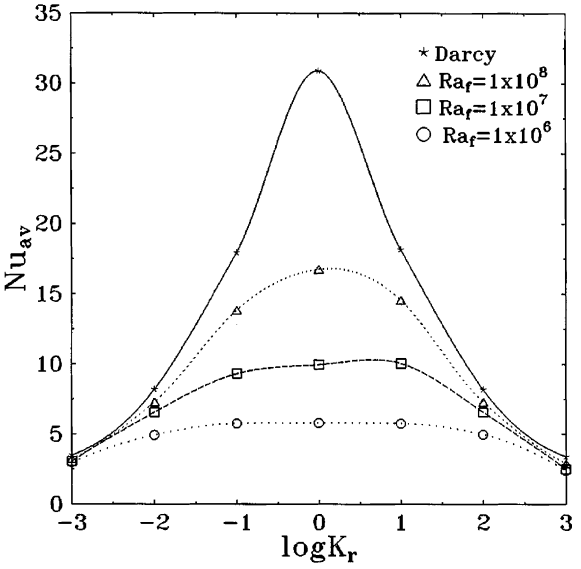

Fig. 8. Variation of Nu_{av} with permeability ratio $Ra_m = 10^5$ for $K_r > 1$ $Ra_m = 10^4$, 100, 10 for $K_r = 0.1$, 0.01, 0.001.

conditions both at the solid walls and at the interface between the two porous media.

Obtained results show that as the difference between permeabilities of the two layers increases, rate of heat transfer decreases. This is the result of decrease in penetration rate from one layer to another. So, maximum heat transfer coefficient is obtained for a single permeability medium. This is because for the investigated range of Rayleigh and Darcy numbers, for a single

medium flow, there exist no permeability gradients at the interface between the two layers and because when permeability is variated, it is equated to a value smaller than a single porosity medium. Also it is important to mention that at high K_r values, heat transfer coefficient decreases because of conduction effects associated with the less permeable medium. Conduction effects are also evident in temperature plots of Fig. 6 (4). Fig. 6 (4) shows that for $K_r = 1000$, heat transfer in layer 2 is conduction dominated. The obtained results show that for design purposes, comparing the investigated range of parameters, and for a constant heat flux enclosure, in order to decrease heat transfer coefficients, instead of filling the enclosure with a single porous medium, only half can be filled with a low permeability medium.

6. Conclusion

Natural convection in a vertically layered porous enclosure is investigated numerically including non-Darcy terms, i.e., general model. The results are presented for flow field and heat transfer for enclosures subjected to constant heat flux from a vertical wall while other vertical wall was kept at a low temperature. The focus of the work was on the validity of the Darcy model when various combinations of fluid Rayleigh number, Darcy number and permeability ratios are considered for fixed values of the modified Rayleigh numbers. It is found that there is significant difference between Darcy model and the general model predictions and the investigated range of parameters show that in most cases, no-slip boundary conditions exist both at the enclosure walls and at the interface between the two porous media. Also for $Ra_f = 1 \times 10^8$, for two different cases, $Da = 1 \times 10^{-4}$, $K_r = 100$ and $Da = 1 \times 10^{-3}$, $K_r = 1000$, two recirculating cells are formed in the enclosure, one being at the center and other in the lower left corner of the enclosure. It was found that for $K_r > 1$, increasing permeability ratio decreases flow penetration from layer 1 to layer 2 while reverse is valid for $K_r < 1$. When permeability gradients are high, because of low penetration rate from/to the less permeable layer and also low velocities within the less permeable layer heat transfer in that layer is conductive. It is also interesting to note that for $Ra_f = 10^7$, $Da = 10^{-6}$ and $K_r = 0.001$, the second layer acts as an enclosure of aspect ratio 2, with a thick left vertical wall, having same conductivity as the effective conductivity of the porous layer.

References

[1] M. Kaviany, Principles of Heat Transfer in Porous Media, Springer, New York, 1994.
[2] D. Nield, A. Bejan, Convection in Porous Media, Springer, New York, 1999.
[3] R. Rana, R.N. Horne, P. Cheng, Natural convection in a multi-layered geothermal reservoir, J. Heat Transfer 101 (1979) 411–416.
[4] P. Cheng, Heat transfer in geothermal systems, Adv. Heat Transfer 14 (1978) 1–105.
[5] R. Rana, Numerical simulation of free convection in a multi-layer geothermal reservoir, M.Sc. Thesis, Department of Mechanical Engineering, University of Hawaii, 1977.
[6] R. McKibbin, M.J. O'Sallivan, Onset of convection in a layered porous medium heated from below, J. Fluid Mech. 96 (1980) 375–393.
[7] R. McKibbin, M.J. O'Sallivan, Heat transfer in a layered porous medium heated from below, J. Fluid Mech. 111 (1981) 141–173.
[8] R. McKibbin, P.A. Tyvand, Anisotropy modelling of thermal convection in multilayered porous media, J. Fluid Mech. 118 (1982) 315–339.
[9] D. Poulikakos, A. Bejan, Natural convection in vertically and horizontally layered porous media heated from the side, Int. J. Heat Mass Transfer 26 (1983) 1805–1814.
[10] F.C. Lai, F.A. Kulacki, Natural convection in layered porous media partially heated from below, Proceedings of the 24th ASME/AIChE National Heat Transfer Conference, Pittsburgh, 1987.
[11] F.C. Lai, F.A. Kulacki, Natural convection across a vertically layered porous cavity, Int. J. Heat Mass Transfer 31 (6) (1988) 1247–1260.
[12] N. Seki, S. Fukusako, H. Inaba, Heat transfer in a confined rectangular cavity packed with porous media, Int. J. Heat Mass Transfer 21 (1987) 985–989.
[13] H. Inaba, M. Sugawara, J. Blumenberg, Natural convection heat transfer in an inclined porous layer, Int. J. Heat Mass Transfer 31 (1988) 1365–1374.
[14] A.A. Mohamad, Spatially fourth order accurate scheme for unsteady convection problems, Numer. Heat Transfer Part B 31 (1977) 373–385.
[15] F.H. Harlow, J.E. Welch, Numerical calculation of time-dependent viscous incompressible flow, Phys. Fluids 8 (1965) 2182–2189.
[16] V. Prasad, F.A. Kulacki, Natural convection in a rectangular porous cavity with constant heat flux on one vertical wall, ASME J. Heat Transfer 106 (1984) 152–157.
[17] A.A. Merrikh, I. Pop, A.A. Mohamad, Transient natural convection in an enclosure filled with a saturated porous medium, Proc. Advances in Comp. Heat Transfer, CHMT-97, Cesme/Turkey, 1997.
[18] C. Beckermann, S. Ramadhyani, R. Viskanta, Natural convection flow and heat transfer between a fluid layer and a porous layer inside a rectangular enclosure, ASME J. Heat Transfer 109 (1987) 363–370.
[19] K. Vafai, R. Thiyagaraja, Analysis of flow and heat transfer at the interface of a porous medium, Int. J. Heat Mass Transfer 30 (7) (1987) 1391–1405.
[20] K. Vafai, S.J. Kim, On the limitation of the Brinkman-Forchheimer-extended Darcy equation, Int. J. Heat and Fluid Flow 16 (1995) 11–15.